Formation and Characterization of the Tetranuclear Scandium Nitride: Sc_4N_4

Yu Gong, YanYing Zhao, and Mingfei Zhou*

Department of Chemistry, Shanghai Key Laboratory of Molecular Catalysts and Innovative Materials, Advanced Materials Laboratory, Fudan University, Shanghai 200433, People's Republic of China

Received: January 31, 2007

The scandium dimer reacts with dinitrogen in solid argon to form the previously characterized planar cyclic $Sc(\mu\text{-}N)_2Sc$ molecule, with the N−N bond being completely cleaved. The cyclic $Sc(\mu\text{-}N)_2Sc$ molecules dimerize on annealing to form a cubic Sc_4N_4 cluster with tetrahedral symmetry, which is a fundamental building block for ScN nanoparticles and crystals.

Introduction

Transition-metal nitrides are technologically important materials and have wide applications. The solid scandium mononitride material has attracted considerable attention. It is believed to be a narrow-gap semiconductor, which has potential application in the fabrication of electronic devices.[1−4] Different experimental methods have been applied for the preparation of scandium nitride.[5−8] The direct reaction of elemental scandium with dinitrogen gas (N_2) at high temperature is an effective way to fabricate single-crystal scandium nitrides.[5,8] The experimental and theoretical modeling of the reactions at the atomic/molecular level is particularly helpful in providing better insight into the mechanism of complex processes in which reactive intermediates are involved. The reactions of Sc atoms with N_2 have been previously investigated using matrix isolation infrared spectroscopy.[9] Some scandium dinitrogen complexes and scandium nitride molecules were observed and characterized. It was found that two Sc atoms can react with N_2 to form the rhombic $Sc(\mu\text{-}N)_2Sc$ molecule, where the N−N bond is completely broken. Interaction of the Sc atom with N_2 has also been the subject of theoretical calculations.[10,11] The $^4\Sigma^-$ state of linear end-on bonded ScNN and the $^4B_1$ state of side-on bonded $Sc(N_2)$ correlate to the first excited-state of the Sc atom and were predicted to be very similar in energy.[9−11]

Recent investigations indicate that some metal dimers are more reactive than metal atoms toward N_2. The titanium dimer reacted with N_2 to form a N−N bond is the completely cleavaged cyclic $Ti(\mu\text{-}N)_2Ti$ molecule without a significant activation barrier.[12−14] The reaction of Gd_2 with N_2 to form cyclic $Gd(\mu\text{-}N)_2Gd$ was observed to proceed via the initial formation of a dinitrogen complex with a simultaneously side-on and end-on bonded N_2. It is interesting to note that the cyclic $Gd(\mu\text{-}N)_2Gd$ molecules can further dimerize to form an unprecedented cubic Gd_4N_4 cluster, which is a fundamental building block for ferromagnetic GdN nanoparticles and crystals.[15] In this paper, we report a matrix isolation infrared spectroscopic and theoretical characterization of a similar multinuclear scandium nitride, Sc_4N_4, which is a species that we show to have a cubic tetrahedral structure and to be a fundamental building block for ScN nanoparticles and crystals.

* Author to whom correspondence should be addressed. E-mail address: mfzhou@fudan.edu.cn.

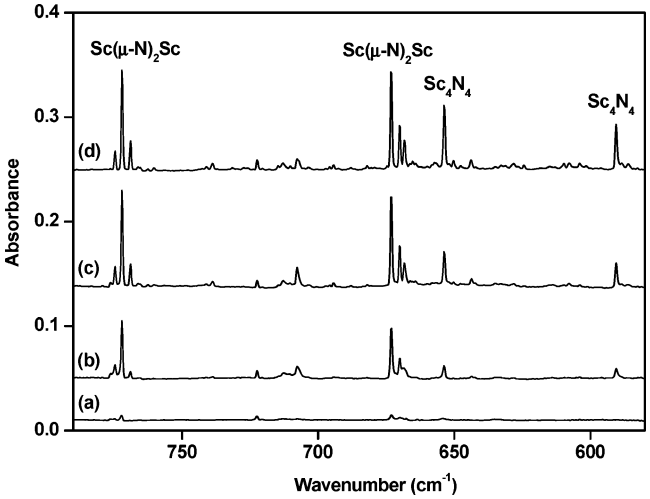

Figure 1. Infrared (IR) spectra in the 790−580 cm^{-1} region from co-deposition of laser-evaporated Sc atoms and clusters with 0.05% N_2 in argon: after 1 h of sample deposition at 6 K (spectrum a), after 25 K annealing (spectrum b) after 35 K annealing (spectrum c), and (d) after 43 K annealing (spectrum d).

Experimental and Computational Methods

The experimental setup for pulsed laser evaporation and matrix isolation infrared absorption spectroscopy has been described in detail previously.[16] Briefly, the 1064 nm Nd:YAG laser fundamental (Continuum, Minilite II, 10 Hz repetition rate and 6 ns pulse width) was focused onto the rotating scandium metal target through a hole in a CsI window. The laser-evaporated Sc atoms and clusters were co-deposited with N_2 in excess argon onto a CsI window that was cooled normally to 6 K by means of a closed-cycle helium refrigerator (ARS, 202N). Generally, matrix samples were deposited for 1−2 h with a gas deposition rate of ∼4 mmol/h. After sample deposition, infrared (IR) spectra were recorded on a Bruker IFS66V spectrometer at a resolution of 0.5 cm^{-1}, using a liquid-nitrogen-cooled HgCdTe (MCT) detector for the spectral range of 4000−470 cm^{-1}. The N_2/Ar mixtures were prepared in a stainless steel vacuum line using standard manometric techniques. Dinitrogen (Shanghai BOC, 99.5%) and $^{15}N_2$ (ISOTEC, 99%) were used to prepare the N_2/Ar mixtures. The $^{14}N_2 + {}^{14}N^{15}N + {}^{15}N_2$ mixture (1:2:1) was prepared via high-frequency discharge of the $^{14}N_2 + {}^{15}N_2$ (1:1) sample.

10.1021/jp070816n CCC: $37.00
Published on Web 06/22/2007

TABLE 1: Infrared Absorptions from the Co-Deposition of Laser-Evaporated Scandium with Dinitrogen in Excess Argon

Infrared Adsorption (cm^{-1})				
$^{14}N_2$	$^{15}N_2$	$^{14}N_2 + {}^{15}N_2$	$^{14}N_2 + {}^{14}N^{15}N + {}^{15}N_2$	assignment
1902.0	1839.0	1902.0, 1839.0	1902.0, 1872.3, 1869.4, 1839.0	ScNN
772.2	752.6	772.2, 752.6	772.2, 762.5, 752.6	$Sc(\mu\text{-}N)_2Sc$
672.9	656.2	672.9, 656.2	672.9, 662.9, 656.2	$Sc(\mu\text{-}N)_2Sc$
653.7	636.9	653.7, 649.6, 645.8, 641.3, 636.9	653.7, 649.6, 647.6, 645.8, 643.4, 641.3, 636.9	Sc_4N_4
590.6	575.4	590.6, 580.5, 575.4	590.6, 584.1, 580.5, 577.8, 575.4	Sc_4N_4

TABLE 2: Calculated Total Energies (after Zero Point Energy (ZPE) Correction), Vibrational Frequencies, and Intensities of the Species Mentioned in the Text

molecule	energy (hartree)	frequency (intensity)[a]
Sc_2 ($^5\Sigma_u^-$)	−1521.258233	258.3 (0)
N_2 ($^1\Sigma_g^+$)	−109.554126	2444.1 (0)
$Sc_2(\mu\text{-}\eta^2\text{:}\eta^1\text{-}N_2)$ ($^1A'$)	−1630.881258	168.1 (11), 331.8 (1), 541.1 (33), 574.6 (4), 632.9 (0), 1226.8 (424)
$Sc_2(\mu\text{-}\eta^2\text{:}\eta^2\text{-}N_2)$ ($^1A_1$)	−1630.900650	201.4 (23), 463.3 (5), 480.9 (0), 545.2 (14), 631.3 (286), 805.8 (78)
$Sc(\mu\text{-}N)_2Sc$ (^1A_g)	−1630.963941	272.8 (128), 440.5 (0), 455.0 (0), 673.4 (294), 758.0 (0), 822.9 (222)
Sc_4N_4 ($^1A_1$)	−3262.205025	344.1 (9), 416.4 (0), 450.5 (0), 460.7 (0), 600.8 (681), 639.7 (0), 686.5 (681)
TS1	−1630.861057	305.2i (7), 177.6 (17), 402.9 (24), 602.4 (79), 667.7 (45), 998.3 (207)
TS2	−1630. 853864	851.8i (834), 178.9 (23), 478.6 (148), 537.4 (48), 706.4 (54), 729.5 (241)

[a] Frequencies are given in units of cm^{-1}, whereas intensity (the value given in parentheses) is presented in terms of km/mol.

Density functional theory (DFT) calculations were performed using the Gaussian 03 program.[17] The three-parameter hybrid functional according to Becke, with additional correlation corrections due to Lee, Yang, and Parr (B3LYP), was utilized.[18] The 6-311+G* basis set was used for the N atom, and the all-electron basis set of Wachters−Hay, as modified by Gaussian, was used for the Sc atom.[19] The geometries were fully optimized, and the stability of the electronic wave function was tested. The harmonic vibrational frequencies were calculated with analytic second derivatives, and zero-point energies (ZPEs) were derived. Transition-state optimizations were performed with the Berny geometry optimization algorithm at the B3LYP/6-311+G* level.

Results and Discussion

The Sc_4N_4 cluster was prepared via the reaction of laser-evaporated scandium with dinitrogen in excess argon. Experiments were performed using different N_2 concentrations and laser energies. With high N_2 concentration (0.5%) and relatively low laser energy, absorptions due to ScNN (1902.0 cm^{-1}) and cyclic $Sc(\mu\text{-}N)_2Sc$ (772.2 and 672.9 cm^{-1}) are the primary products upon sample deposition, which have been previously identified.[9] The $Sc(NN)_x$ complexes and the N_2-ligated $(NN)_x\text{-}Sc(\mu\text{-}N)_2Sc(NN)_x$ complex absorptions markedly increased on annealing. The experiments with low N_2 concentrations and high laser energies are of particular interest here. The IR spectra in the 790−580 cm^{-1} region with 0.05% N_2 in argon and a laser energy of 15 mJ/pulse are shown in Figure 1, and the product absorptions are listed in Table 1. The cyclic $Sc(\mu\text{-}N)_2Sc$ absorptions were observed to increase when subjected to annealing at 25 and 35 K; however, the N_2-ligated $(NN)_xSc\text{-}(\mu\text{-}N)_2Sc(NN)_x$ complex absorptions were barely observed, even after high-temperature annealing. Two new absorptions, at 653.7 and 590.6 cm^{-1}, appear together when subjected to annealing at 25 K, and increase markedly when subjected to annealing at 35 and 43 K. Very weak absorptions due to ScO, $[ScO(Ar)_5]^+$, and ScO_2^- were also observed.[20,21] In the N−N stretching frequency region (not shown in Figure 1), no obvious absorptions except weak ScNN and (η^1-NN)Sc(H)OH (1884.4 cm^{-1}) absorptions were observed.[22]

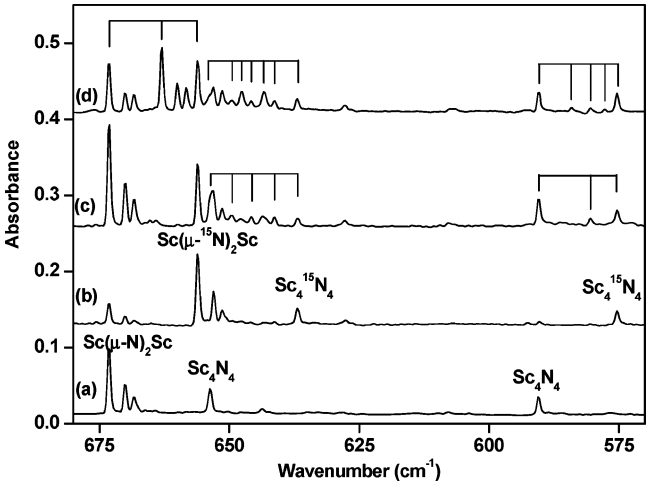

Figure 2. IR spectra in the 680−570 cm^{-1} region from co-deposition of laser-evaporated Sc atoms and clusters with isotopic labeled N_2 in excess argon. Spectra were taken after 1 h of sample deposition, followed by 35 K annealing: 0.05% $^{14}N_2$ (spectrum a), 0.05% $^{15}N_2$ (spectrum b), 0.03% $^{14}N_2$ + 0.03% $^{15}N_2$ (spectrum c), and (d) 0.015% $^{14}N_2$ + 0.03% $^{14}N^{15}N$ + 0.015% $^{15}N_2$ (spectrum d).

The experiments were repeated, using the isotopically labeled $^{15}N_2$ and the ($^{14}N_2 + {}^{15}N_2$) and ($^{14}N_2 + {}^{14}N^{15}N + {}^{15}N_2$) mixtures. The isotopic counterparts are also listed in Table 1. The spectra in the 680−570 cm^{-1} region with different isotopic samples are shown in Figure 2.

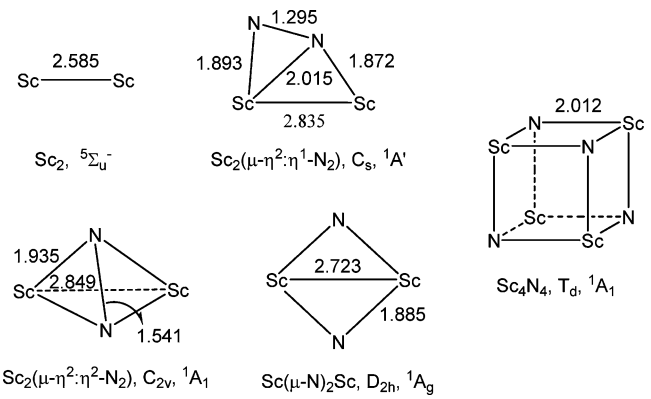

Figure 3. Optimized structures of the Sc_2, Sc_2N_2, and Sc_4N_4 molecules. (Bond lengths given in angstroms, bond angles given in degrees.)

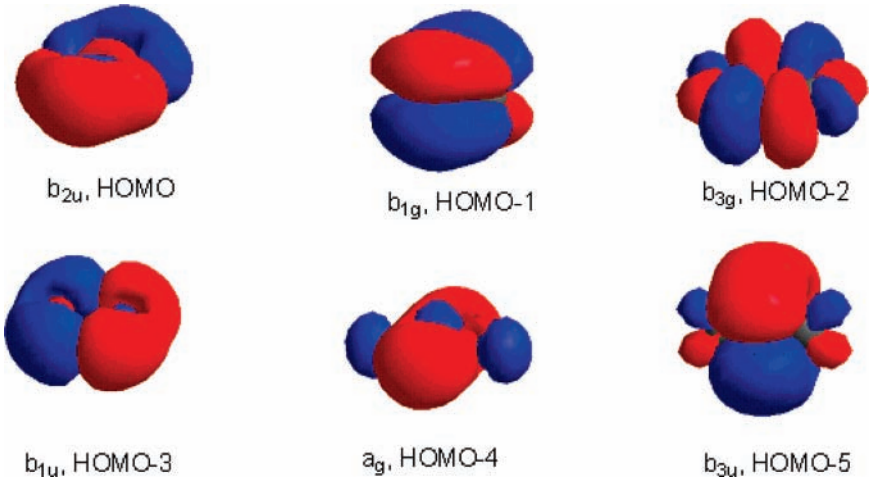

Figure 4. Molecular orbital contour surfaces for the six highest-energy occupied orbitals of Sc(μ-N)$_2$Sc.

The 653.7 and 590.6 cm^{-1} absorptions were barely observed in experiments that involved high N_2 concentrations, but were observed to increase markedly when subjected to annealing in experiments that involved low N_2 concentrations and high laser energies. When a $^{15}N_2$ sample was used, the 653.7 and 590.6 cm^{-1} absorptions shifted to 636.9 and 575.4 cm^{-1}, respectively. The isotopic $^{14}N/^{15}N$ ratios of 1.0264 for both modes indicate that these absorptions are due to Sc−N stretching vibrations. In the experiment with equimolar mixture of $^{14}N_2$ and $^{15}N_2$, the low mode splits into a triplet at 590.6, 580.5, and 575.4 cm^{-1} with the intermediate absorption lower in intensity than the pure isotopic counterparts, as shown in trace c in Figure 2. In the experiment with a 1:2:1 mixture of $^{14}N_2 + {}^{14}N^{15}N + {}^{15}N_2$ (trace d in Figure 2), a quintet with three weak intermediates, at 584.1, 580.5, and 577.8 cm^{-1}, was produced for the low mode. These spectral features indicate that the 590.6 cm^{-1} band is due to a triply degenerate Sc−N stretching mode of a tetrahedral molecule with four equivalent N atoms, which result from two equivalent N_2 molecules. The upper mode splits into a quintet with three weak intermediates, at 649.6, 645.8, and 641.3 cm^{-1}, with the equimolar mixture of $^{14}N_2$ and $^{15}N_2$; meanwhile, two extra intermediate absorptions, at 647.6 and 643.4 cm^{-1}, were resolved in the experiment with the 1:2:1 mixture of $^{14}N_2 + {}^{14}N^{15}N + {}^{15}N_2$. The aforementioned experimental observations suggest the assignment of the 653.7 and 590.6 cm^{-1} absorptions to a Sc_4N_4 species with a tetrahedral structure.

To validate the experimental assignment, DFT calculations were performed on the experimentally identified molecules. Calculations were first conducted on the ScNN molecule, which was predicted to have a $^4\Sigma^-$ ground state with Sc−N and N−N bond lengths of 2.036 and 1.142 Å, respectively, and N−N stretching frequency of 1944.8 cm^{-1}. In agreement with previous calculations,[9] the cyclic Sc(μ-N)$_2$Sc molecule was predicted to have a ^1A_g ground state with a D_{2h} symmetry (see Figure 3). The lowest triplet state ($^3B_{2u}$) was calculated to be 27.0 kcal/mol higher in energy than the singlet ground state. The ^1A_g ground state has the following electron configuration:

$$(\text{core})(b_{3u})^2(a_{1g})^2(b_{1u})^2(b_{3g})^2(b_{1g})^2(b_{2u})^2$$

The valence molecular orbitals are illustrated in Figure 4. The HOMO, HOMO-2, HOMO-3, and HOMO-4 orbitals are σ-bonding orbitals; the HOMO-1 b_{1g} orbital is a δ-bonding orbital that is comprised of Sc d_{xy} and N p_x atomic orbitals (assuming the molecular plane to be the *yz* plane); the HOMO-5 b_{3u} orbital is a π-bonding orbital. The molecule can be viewed as having four Sc−N σ bonds and two delocalized three-center two-electron (3c2e) (d−p−d) bonds. Hence, each Sc−N bond can be regarded as having a bond order of 1.5. The Sc−N bond length was predicted to be 1.885 Å, which is significantly shorter than the typical Sc−N single bond.[23] The N−N separation was computed to be 2.606 Å, which indicates that there is no direct bonding interaction between the two N atoms. The two experimentally observed mode of the ground state Sc(μ-N)$_2$Sc molecule were calculated at 822.9 and 673.4 cm^{-1} (Table 2).

The Sc_4N_4 cluster was predicted to have a $^1A_1$ ground state with a T_d symmetry (see Figure 3). The Sc−N and Sc−Sc bond distances were computed to be 2.012 and 2.888 Å, respectively. The $^1A_1$ ground state Sc_4N_4 cluster was calculated to have two strong triply degenerate Sc−N stretching modes (T_2) at 686.5 and 600.8 cm^{-1} with almost-equal IR intensities. The corresponding $Sc_4{}^{15}N_4$ absorptions were computed at 668.4 and 584.7 cm^{-1}. When two ^{14}N atoms in Sc_4N_4 were substituted by isotopic labeled ^{15}N, the triply degenerate mode becomes nondegenerate. The upper mode splits into three absorptions at 682.1, 677.8, and 673.1 cm^{-1} with approximately the same IR intensities; the low mode also splits into three absorptions, at 600.8, 590.7, and 584.7 cm^{-1}. Therefore, a quintet isotopic feature with ~3:2:2:2:3 relative intensities for the upper mode and a triplet with ~5:2:5 relative intensities for the low mode should be observed when a 1:1 mixed $^{14}N_2 + {}^{15}N_2$ sample was used, which are in excellent agreement with the experimental observations. The isotopic spectral features are more complicated when a 1:2:1 mixture of $^{14}N_2 + {}^{14}N^{15}N + {}^{15}N_2$ was used. According to the calculations, the low mode should split into a quintet with ~17:4:6:4:17 relative intensities, whereas the upper mode should split into seven absorptions with 7:6:8:6:8:6:7 relative intensities, which also is consistent with the experimental observations.

The experimental observations suggest that the cubic Sc_4N_4 cluster was formed by dimerization of the Sc(μ-N)$_2$Sc molecules, which were produced via the reaction of the scandium dimer with dinitrogen. The ground state of the scandium dimer has been established to be $^5\Sigma_u^-$.[24,25] Our DFT calculations also predicted $^5\Sigma_u^-$ to be the ground state, with a Sc−Sc distance of 2.585 Å, in agreement with the previous calculations.[26] As shown in Figure 5, the reaction of $Sc_2 + N_2$ to form the cyclic Sc(μ-N)$_2$Sc molecule proceeds via two intermediates. The initial step of the reaction is the formation of a $Sc_2(\mu\text{-}\eta^2{:}\eta^1\text{-}N_2)$ complex, which was predicted to have a $^1A'$ ground state with a planar C_s structure. This association reaction requires spin crossing and is predicted to be exothermic by 43.2 kcal/mol

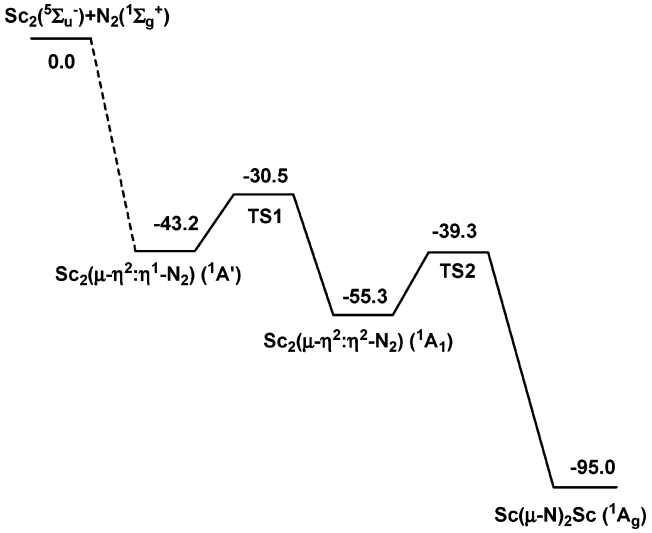

Figure 5. Potential energy profile for the $Sc_2 + N_2 \rightarrow Sc(\mu\text{-}N)_2Sc$ reaction. Energies given are given in kcal/mol. The dashed line indicates the computationally unexplored spin-crossing area.

from the ground state Sc_2 ($^5\Sigma_u^-$) and N_2 ($^1\Sigma_g^+$). The $Sc_2(\mu\text{-}\eta^2\text{:}\eta^1\text{-}N_2)$ intermediate has a side-on and end-on bonded N_2, which is drastically activated with a remarkably long N−N bond. The N−N bond dissociation reaction from the $Sc_2(\mu\text{-}\eta^2\text{:}\eta^1\text{-}N_2)$ complex to form the cyclic $Sc(\mu\text{-}N)_2Sc$ isomer is exothermic (by 51.8 kcal/mol) and proceeds via a bridge-bonded C_{2v} intermediate lying 12.1 kcal/mol lower in energy than the $Sc_2(\mu\text{-}\eta^2\text{:}\eta^1\text{-}N_2)$ complex. The reaction proceeds via a transition state (TS1) lying 12.7 kcal/mol higher in energy than the $Sc_2(\mu\text{-}\eta^2\text{:}\eta^1\text{-}N_2)$ complex. Because the formation of $Sc_2(\mu\text{-}\eta^2\text{:}\eta^1\text{-}N_2)$ from $Sc_2 + N_2$ is initially exothermic by 43.2 kcal/mol, which significantly surmounts the energy barrier for the N−N bond breaking reaction, the formation of cyclic $Sc(\mu\text{-}N)_2Sc$ is spontaneous in solid argon. Neither the $Sc_2(\mu\text{-}\eta^2\text{:}\eta^1\text{-}N_2)$ complex nor the bridge-bonded C_{2v} intermediate was observed in the experiments. Recent studies reported that the ground state titanium dimer reacted with dinitrogen to form the cyclic $Ti(\mu\text{-}N)_2Ti$ molecule spontaneously in solid neon and argon matrixes.[12−14] However, the $Gd_2(\mu\text{-}\eta^2\text{:}\eta^1\text{-}N_2)$ complex was experimentally observed in the $Gd_2 + N_2$ reaction.[15]

The Sc_4N_4 cluster is formed by fusing the δ- and π-bonds of two cyclic $Sc(\mu\text{-}N)_2Sc$ compounds. This dimerization reaction is predicted to be barrierless and exothermic (by 173.7 kcal/mol). The reaction of cyclic $Sc(\mu\text{-}N)_2Sc$ with N_2 to form the $(NN)_xSc(\mu\text{-}N)_2Sc(NN)_x$ complex is in competition with the dimerization reaction in a solid argon matrix. In the experiments with high N_2 concentrations, the formation of the N_2-ligated complex dominates, whereas in the experiments with low N_2 concentrations and high laser energy, the dimerization reaction dominates. Because of the availability of lone pairs on N atoms and empty d-orbitals on Sc atoms, the cubic Sc_4N_4 with tetrahedral symmetry is a perfect building block of the bulk ScN crystal, which has a rocksalt structure.

Conclusions

Co-condensation of laser-evaporated Sc atoms and clusters with dinitrogen in excess argon at 6 K produces the previously characterized cyclic $Sc(\mu\text{-}N)_2Sc$ absorptions, which increase when subjected to annealing. In the experiments with low N_2 concentration and high laser energy, the cyclic $Sc(\mu\text{-}N)_2Sc$ molecules further dimerize to form the Sc_4N_4 cluster, which is characterized to have a cubic structure with a tetrahedral symmetry. The Sc_4N_4 cluster is a fundamental building block of ScN nanoparticles and crystals, which have a rocksalt structure. The reaction path from the scandium dimer and the dinitrogen, leading to the observed products, is also calculated and discussed.

Acknowledgment. This work is supported by NKBRSF (No. 2004CB719501) and NNSFC (No. 20433080) of China.

References and Notes

(1) Takeuchi, N. *Phys. Rev., B* **2002**, *65*, 045204.
(2) Farrer, N.; Bellaiche, L. *Phys. Rev., B* **2002**, *66*, 201203R.
(3) Šimůnek, A.; Vackář, J.; Kunc, K. *Phys. Rev., B* **2005**, *72*, 045110.
(4) Ranjan, V.; Bellaiche, L.; Walter, E. J. *Phys. Rev. Lett.* **2003**, *90*, 257602.
(5) Lengauer, W. *J. Solid-State Chem.* **1988**, *76*, 412.
(6) Dismukes, J. P.; Yin, W. M.; Ban, V. S. *J. Cryst. Growth* **1972**, *13/14*, 365.
(7) Karl, M.; Seybert, G.; Massa, W.; Dehnicke, K. *Z. Anorg. Allg. Chem.* **1999**, *625*, 375.
(8) Niewa, R.; Zherebtsov, D. A.; Kirchner, M.; Schmidt, M.; Schnelle, W. *Chem. Mater*. **2004**, *16*, 5445.
(9) Chertihin, G. V.; Andrews, L.; Bauschlicher, C. W., Jr. *J. Am. Chem. Soc.* **1998**, *120*, 3205.
(10) Pilme, J.; Silvi, B.; Alikhani, M. E. *J. Phys. Chem. A* **2005**, *109*, 10028.
(11) Kardahakis, S.; Koukounas, C.; Mavridis, A. *J. Chem. Phys.* **2006**, *124*, 104306.
(12) Himmel, H. J.; Hübner, O.; Klopper, W.; Manceron, L. *Angew. Chem., Int. Ed.* **2006**, *45*, 2799.
(13) Himmel, H. J.; Hübner, O.; Bischoff, F. A.; Klopper, W.; Manceron, L. *Phys. Chem. Chem. Phys.* **2006**, *8*, 2000.
(14) Kuganathan, N.; Green, J. C.; Himmel, H. J. *New J. Chem*. **2006**, *30*, 1253.
(15) Zhou, M. F.; Jin, X.; Gong, Y.; Li, J. *Angew. Chem., Int. Ed*. **2007**, *46*, 2911.
(16) (a) Zhou, M. F.; Zhang, L. N.; Dong, J.; Qin, Q. Z. *J. Am. Chem. Soc.* **2000**, *122*, 10680. (b) Wang, G. J.; Gong, Y.; Chen, M. H.; Zhou, M. F. *J. Am. Chem. Soc.* **2006**, *128*, 5974.
(17) Frisch, M. J.; Trucks, G. W.; Schlegel, H. B.; Scuseria, G. E.; Robb, M. A.; Cheeseman, J. R.; Montgomery, J. A., Jr.; Vreven, T.; Kudin, K. N.; Burant, J. C.; Millam, J. M.; Iyengar, S. S.; Tomasi, J.; Barone, V.; Mennucci, B.; Cossi, M.; Scalmani, G.; Rega, N.; Petersson, G. A.; Nakatsuji, H.; Hada, M.; Ehara, M.; Toyota, K.; Fukuda, R.; Hasegawa, J.; Ishida, M.; Nakajima, T.; Honda, Y.; Kitao, O.; Nakai, H.; Klene, M.; Li, X.; Knox, J. E.; Hratchian, H. P.; Cross, J. B.; Bakken, V.; Adamo, C.; Jaramillo, J.; Gomperts, R.; Stratmann, R. E.; Yazyev, O.; Austin, A. J.; Cammi, R.; Pomelli, C.; Ochterski, J. W.; Ayala, P. Y.; Morokuma, K.; Voth, G. A.; Salvador, P.; Dannenberg, J. J.; Zakrzewski, V. G.; Dapprich, S.; Daniels, A. D.; Strain, M. C.; Farkas, O.; Malick, D. K.; Rabuck, A. D.; Raghavachari, K.; Foresman, J. B.; Ortiz, J. V.; Cui, Q.; Baboul, A. G.; Clifford, S.; Cioslowski, J.; Stefanov, B. B.; Liu, G.; Liashenko, A.; Piskorz, P.; Komaromi, I.; Martin, R. L.; Fox, D. J.; Keith, T.; Al-Laham, M. A.; Peng, C. Y.; Nanayakkara, A.; Challacombe, M.; Gill, P. M. W.; Johnson, B.; Chen, W.; Wong, M. W.; Gonzalez, C.; Pople, J. A. *Gaussian 03*, revision B.05; Gaussian, Inc.: Wallingford, CT, 2004.
(18) (a) Becke, A. D. *J. Chem. Phys.* **1993**, *98*, 5648. (b) Lee, C.; Yang, W.; Parr, R. G. *Phys. Rev., B* **1988**, *37*, 785.
(19) (a) McLean, A. D.; Chandler, G. S. *J. Chem. Phys*. **1980**, *72*, 5639. (b) Krishnan, R.; Binkley, J. S.; Seeger, R.; Pople, J. A. *J. Chem. Phys*. **1980**, *72*, 650.
(20) (a) Chertihin, G. V.; Andrews, L.; Rosi, M.; Bauschlicher, C. W., Jr. *J. Phys. Chem. A* **1997**, *101*, 9085. (b) Bauschlicher, C. W., Jr.; Zhou, M. F.; Andrews, L.; Johnson, J. R. T.; Panas, I.; Snis, A.; Roos, B. O. *J. Phys. Chem. A* **1999**, *103*, 5463.
(21) (a) Zhao, Y. Y.; Wang, G. J.; Chen, M. H.; Zhou, M. F. *J. Phys. Chem. A* **2005**, *109*, 6621. (b) Zhao, Y. Y.; Gong, Y.; Chen, M. H.; Ding, C. F.; Zhou, M. F. *J. Phys. Chem. A* **2005**, *109*, 11765.
(22) Chen, M. H.; Wang, G. J.; Jiang, G. Y.; Zhou, M. F. *J. Phys. Chem. A* **2005**, *109*, 415.
(23) Knight, L. K.; Piers, W. E.; Lessard, P. F.; Parvez, M.; McDonald, R. *Organometallics* **2004**, *23*, 2087.
(24) Knight, L. B., Jr.; Van Zee, R. J.; Weltner, W., Jr. *Chem. Phys. Lett.* **1983**, *94*, 296.
(25) Papai, I.; Castro, M. *Chem. Phys. Lett.* **1997**, *267*, 551.
(26) Gutsev, G. L.; Bauschlicher, C. W., Jr. *J. Phys. Chem. A* **2003**, *107*, 4755.